International Journal of Scientific Engineering and Technology (ISSN : 2277-1581)
Volume No.2, Issue No.7, pp : 651-655 1 July 2013

Segmentation of Renal Calculi Using Squared Euclidean Distance Method

Dr. P. R. Tamiselvi
School of Computer Technology and Applications, Kongu Engineering College
Perundurai-638 052, Tamilnadu, India
Email: selvipr2003@gmail.com

Abstract—In this proposed Contour based Squared Euclidean Distance (CSED) segmentation method, initially the preprocessing techniques are applied to reduce the noise from the ultra sound kidney images. Then Squared Euclidean Distance (SED) is determined between the training image centroid values and the selected regions centroid values. In addition, the usage of ANFIS in supervised learning has made the technique more efficient than the previous techniques. Thus the obtained error is minimized when compared to the existing algorithm that leads to high efficiency.

Keywords— Ultrasound Kidney Images- Segmentation- Expert outlined curve- Squared Euclidean Distance

I. Introduction

The most common troubles that occur in the human urinary system is renal calculi, which is often called as kidney stones or urinary stones [i]. Normally, any person affected by these kidney stone diseases will suffer from considerable pain which leads to abnormal kidney function, and also the mechanism for this disease is poorly understood so far [ii]. Kidney is the most salient organ in the urinary system, which not only produce urine but also helpful in purifying the blood. The two important functions of kidney: (i) Removing harmful substances from the blood, and (ii) Keeping the useful components in proper balance. Kidney stones appear in diverse varieties, among which the four basic types that found more often are Calcium-containing stones, Uric acid stones, Struvite or infected stones and Cystine stones [vii]. Normally the kidney diseases are classified as hereditary, congenital or acquired **[x].** The detection of calcifications inside the body is a large field of study including several dynamic areas of research, which is mainly useful for diagnosing the kidney stone diseases. The actual kidney stones may be rough non-spherical in shape, but the dominant effects that are used to find the fracture in actual kidney stones, are based on the reverberation time across the length of the stone **[xi].**

Due to the occurrence of dominant speckle noise and attenuated artifacts in abdominal ultrasound images, the segmentation of stones from these images is very complex and challenging **[viii]**. Hence, this task is performed by the use of much prior information such as texture, shape, spatial location of organs and so on. Several automatic and semiautomatic methods have been proposed. Even though the performance such methods are better when the contrast-to-noise ratio is high, it deteriorates quickly when the structures are insufficiently defined and have low contrast like the neuroanatomic structures, such as thalamus, globus pallidus, putamen, etc. [iv]. The X-ray, positron emission tomography (PET), computer tomography (CT), Ultrasound (US) and magnetic resonance imaging (MRI) are the widely available different medical imaging modalities which are broadly employed in regular clinical practice **[5]**. As compared to other medical imaging modalities such as computed tomography (CT) and magnetic resonance imaging (MRI), the US is particularly difficult to segment because the quality of the image is almost low than the CT and MRI [iii]. Ultrasound (US) image segmentation is greatly depends on the quality of data [vi]. Moreover, it is complex to extract the features that represent the kidney tissues by segmenting the kidney region **[x].** Although, ultrasound imaging is widely utilized in the medical field **[ix]**

US imaging is popular in the field of medicine not only due to its economical cost and non-invasive nature, but also it is a radiation-free imaging technique **[viii]**. US imaging is economical and simple to use and also provides a faster and more exact procedures due to its real time capabilities. In numerous applications, an important role is played by the precise identification of organs or objects that are present in US images [iii].

II. Material and Methodology

The proposed renal calculi segmentation method consists of three major steps namely, (i) Determining the region parameters (ii) Region selection using contour method and (iii) Finding distinction between centroids by utilizing Squared Euclidean Distance (SED). The proposed renal calculi CSED segmentation training and testing procedure is shown in Figure 1.

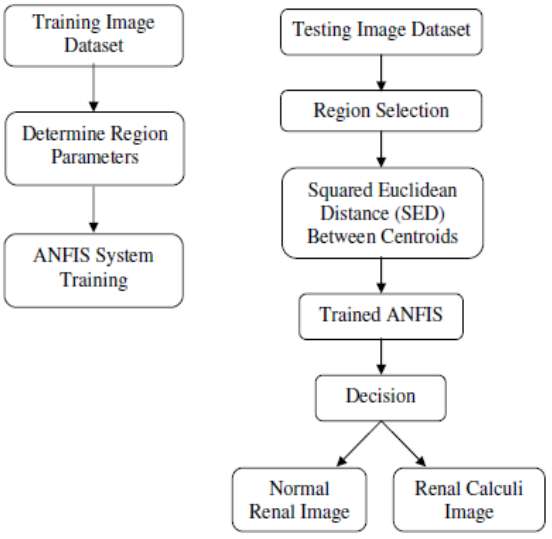

Figure 1: Proposed CSED segmentation training and testing procedure

2.1 Determine Region Parameters

Then, we determine the region parameters for the extracted regions from R by utilizing MATLAB function. The region parameters determined for each region are (i) Area (ii) Centroid (iii) Orientation and (iv) Bounding Box. This region parameter values are given to the ANFIS system for training process. In training process, the normal and calculi area is identified by the threshold values t_1 and t_2. The ANFIS system result value is represented as x. The final decision is defined by normal and calculi

2.2 Region Selection Using Contour Method

Region selection process performed using renal calculi images are taken from the testing image dataset $D^t = \{I_1^t, I_2^t, \cdots I_n^t\}; n = 1 \cdots N^t$, where N represents the total number of renal calculi images in the dataset D^t. The dataset D^t contains the images that are in the dimension of $P \times Q$; $1 \le p \le P, 1 \le q \le Q$. To accomplish the region selection process, we utilized a contour method.

Contour method: Contour method [21] is used to find the boundary of objects in images. Initially, contour method finds the contour plot of the given gray scale image I_C. The contour method function is described in the following equation 1.

$$I_C = (I_n^t, k) \qquad (1)$$

Where, I_C represents the result of the contour method renal calculi gray scale image, I_C is an input renal calculi gray scale image and k is the number of evenly spaced contour levels in the plot. If you neglect the argument, the number of levels and the values of the levels are selected automatically. Contour method automatically sets the axis so their orientation and aspect ratio match the image.

After that, we select the last group values from the contour method result image I_n^{tc}. This group values contains some regions, we calculates the region parameters for that regions and the region parameters values are given to the ANFIS system that are referred in section 3.1. Then we choose few numbers of regions from the image I_n^{tc} which are greater than the threshold value t_1 and this selected region values are given to the empty mask S. The mask S contains m^s number of regions, which is represented as $R^s = \{r_1^s, r_2^s, \cdots r_{m^s}^s\}, m^s = 1 \cdots M^s$. Next, we compute the centroid values for the regions R^s in the mask S, it is represented as $C^s(x,y) = \{c_1^s(x,y), c_2^s(x,y), \cdots c_{m^s}^s(x,y)\}$.

2.3 Find distinction between centroids by utilizing Squared Euclidean Distance (SED)

There are m^s number of regions in the mask S, these mask regions are not optimal to find the exact calculi from the images. So we find the optimal regions among the available regions in S by exploiting Squared Euclidean Distance (SED) between the regions. SED is computed between the x coordinates regions centroid values $C^s(x,y)$ and training images centroid values $C(x,y)$ and y coordinates regions centroid values $C^s(x,y)$ and training images centroid values $C(x,y)$ values individually. The SED difference process is described in the following equ.2&3 for both x and y coordinates values.

$$\varphi(x) = (c_1^{I_1}(x) - c_1^s(x))^2 + \cdots (c_n^{I_n}(x) - c_{m^s}^s(x))^2 \text{ ----- (2)}$$

$$\varphi(y) = (c_1^{I_1}(y) - c_1^s(y))^2 + \cdots (c_n^{I_n}(y) - c_{m^s}^s(y))^2 \text{ -----(3)}$$

The values $\varphi(x)$ and $\varphi(y)$ are compared with the threshold value t_3. If any one of the result values $\varphi(x)$ or $\varphi(y)$ are greater than the given threshold value t_3, that corresponding region are selected. Then this selected optimal region values are put into the equivalent testing image in dataset D^t.

By performing all the above described process in various renal calculi kidney images, the calculi region is segmented.

III. Results and Tables

The CSED segmentation technique is implemented in MATLAB platform and it is evaluated using 30 medical ultra sound renal images, which are collected from various medical diagnosis centers. In 30 images, 15 images are normal renal images and 15 are renal calculi images. The ANFIS system has utilized 66% of images for the training process and 33% of images for the testing process. In the proposed CSED segmentation method, three major steps are performed over these training and testing renal calculi and renal ultra sound images. The sample input normal and calculi images are shown in figure 2.

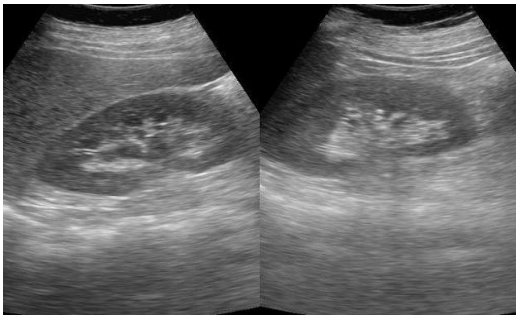

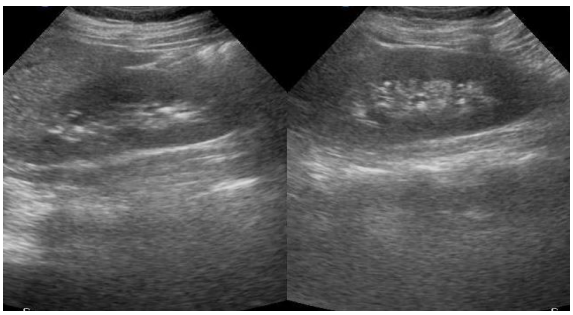

(i) (ii)

Figure 2: Sample Input Renal Images (i) Normal Renal Image (ii) Renal Image with Calculi

The region parameter values are computed for the 66% training images and these parameters result values are given to the ANFIS system to perform the training process. The region parameters values are well trained in the ANFIS system and this performance is evaluated with testing renal calculi images. The 33% of testing images are involved the process of region selection and SED is computed between the region centroid values. The following figure 3 shows the contour method results of renal calculi image. The result images shows that the contour method has divided the testing image pixels into three groups by representing three different colors.

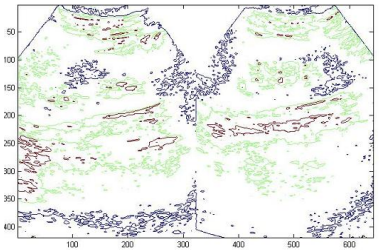

Figure 3: Contour Method Result of Renal Image with Calculi

The selected group value from the contour method result is shown in figure 4. After the region parameters calculation for the regions is shown in fig 4, the parameters are given to the ANFIS; the ANFIS system result with the threshold value, the selected regions placed in the new empty mask are shown in figure 5. Then the centroid values for these regions shown in fig 5 are calculated. The result of the optimal regions selection process by SED is shown in figure 6.

Figure 4: Renal Calculi Image Selected Group Value Result from the Contour Method

Figure 5: The New Mask Selected Regions

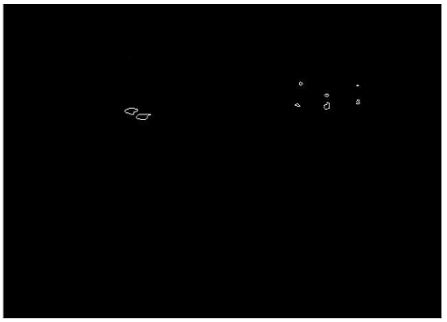

Figure 6: Regions after the SED Process

In figure 7, the calculi regions are exactly marked in red color. The result image has shown that the proposed CSED segmentation method has exactly found the calculi region from the renal calculi images. The performance of proposed CSED segmentation method is analyzed with different images and it is described in the following section.

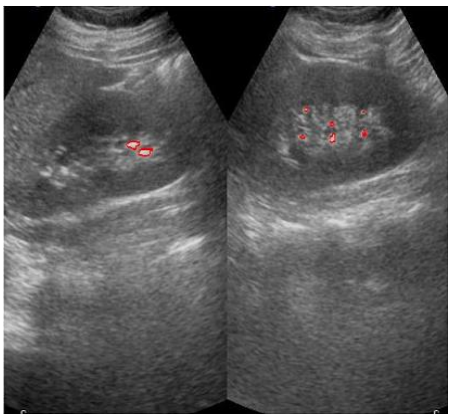

Figure 7: Final Output of the Proposed CSED Segmentation Result

4.1 Performance Analysis

The performance of the CSED segmentation method is evaluated by utilizing five testing images. This performance analysis exploits statistical measures [xii], to compute the accuracy of calculi segmentation done by the CSED segmentation method. The performance of the CSED segmentation analysis is shown in the below Table 1.

Image ID	Sensitivity	Specificity	Accuracy	MCC
1	99.88	68.16	99.78	67.41
2	99.92	34.97	99.72	44.43
3	99.94	36.80	99.77	47.62
4	99.97	28.48	99.89	38.71
5	99.94	51.76	99.88	51.53

Table 1: Statistical performance measures for five different US renal calculi

The segmented stone area by CSED segmentation method is compared with previous IORM segmentation method and conventional segmentation algorithms. A relative error is calculated between the segmented stone area marked by the expert radiologist and the proposed method. The formula for the calculation of relative error is described below,

$$\nu = \left| \frac{E - P}{E} \right| \times 100 \quad (4)$$

Where, ν - Relative Error

E - Stone area marked by Expert radiologist

P - Stone area marked by the proposed CSED segmentation method

The stone area marked by the expert radiologist, the CSED segmentation method and its relative error are given in Table 2.

Expert radiologist (mm^2)	Stone area (mm^2)	Relative error of CSED method
51.59	51.59	0.00
17.20	17.20	0.00
24.61	24.61	0.00
12.70	12.70	0.00
22.75	22.75	0.00
24.34	24.34	0.00
13.23	13.23	0.00
9.26	9.26	0.00

Table 2: CSED segmentation relative error performance

The relative error performance of CSED segmentation method is compared with conventional algorithms values that are shown in the Table 3

Image ID	Relative error of CSED	Relative error existing	Relative error existing
	method	algorithm I	algorithm II
1	0.00	2.180	1.557
2	0.00	3.142	2.243
3	0.00	1.441	0.153
4	0.00	1.038	0.692
5	0.00	0.908	0.893
6	0.00	9.207	0.929
7	0.00	0.381	0.198
8	0.00	0.370	0.192
Mean	0.00	2.333	0.857

Table 3: Comparison result of CSED segmentation relative error with IORM method and existing algorithm (I&II) performance

The relative error of CSED segmentation is 100% lower than the conventional segmentation algorithms and it also given a more mean accurate stone area calculation than the existing IORM method.

IV. Conclusion

The proposed method was implemented and set of renal calculi images were utilized to evaluate the proposed segmentation method. The method has exactly detected the calculi and produced a high segmentation accuracy result when compared to the existing segmentation method. The proposed method has produced less relative error than the existing method relative error performance. Moreover, our proposed CSED segmentation method has produced 99% of accuracy and 100% of relative error performance than the existing algorithms.

References

i. *Ioannis Manousakas, Chih-Ching Lai and Wan-Yi Chang, "A 3D Ultrasound Renal Calculi Fragmentation Image Analysis System for Extracorporeal Shock Wave Lithotripsy", International Symposium on Computer, Communication, Control and Automation, Vol. 1, pp. 303-306, 2010*

ii. *Jie-Yu He, Sui-Ping Deng and Jian-Ming Ouyang, "Morphology, Particle Size Distribution, Aggregation, and Crystal Phase of Nanocrystallites in the Urine of Healthy Persons and Lithogenic Patients, " IEEE Transactions On Nanobioscience, Vol. 9, No. 2, pp. 156-163, June 2010*

iii. *Jun Xie, Yifeng Jiang and Hung-tat Tsui, "Segmentation of Kidney From Ultrasound Images Based on Texture and Shape Priors", IEEE Transactions On Medical Imaging, Vol. 24, No. 1, pp. 45-56, January 2005*

iv. *Ujjwal Maulik, "Medical Image Segmentation Using Genetic Algorithms", IEEE Transactions On Information Technology In Biomedicine, Vol. 13, No. 2, pp. 166-173, March 2009*

v. *Mahmoud Ramze Rezaee, Pieter M. J. van der Zwet, Boudewijn P. F. Lelieveldt, Rob J. van der Geest and Johan H. C. Reiber, "A Multiresolution Image Segmentation Technique Based on Pyramidal Segmentation and Fuzzy Clustering", IEEE Transactions On Image Processing, Vol. 9, No. 7, pp. 1238-1248, July 2000*

vi. *Alison Noble and Djamal Boukerroui, "Ultrasound Image Segmentation: A Survey", IEEE Transactions on Medical Imaging, Vol. 25, No. 8, pp. 987-1010, August 2006*

vii. *Saurin R. Shah, Manhar D. Desai and Lalit Panchal, "Identification of Content Descriptive Parameters for Classification of Renal Calculi", International Journal of Signal and Image Processing, Vol.1, No. 4, pp. 255-259, 2010*

viii. *Abhinav Gupta, Bhuvan Gosain and Sunanda Kaushal, "A Comparison of Two Algorithms for Automated Stone Detection in Clinical B-Mode Ultrasound Images Of the Abdomen", Journal of Clinical Monitoring and Computing, Vol. 24, pp. 341–362, 2010*

ix. *Ratha Jeyalakshmi and Ramar Kadarkarai,"Segmentation and feature extraction of fluid-filled uterine fibroid-A knowledge-based approach ", Maejo International Journal of Science and Technology, Vol. 4, No. 3, pp. 405-416, 2010*

x. *K. Bommanna Raja · M. Madheswaran and K. Thyagarajah, "Texture pattern analysis of kidney tissues for disorder identification and classification using dominant Gabor wavelet", Journal Machine Vision and Applications, Vol. 21, No. 3, pp. 287-300, 2010*

xi. *Ioannis Manousakas, Yong-Ren Pu, Chien-Chen Chang and Shen-Min Liang, "Ultrasound Image Analysis for Renal Stone Tracking During Extracorporeal Shock Wave Lithotripsy", In Proceedings of IEEE EMBS Annual International Conference, New York City, USA, pp. 2746-2749, 2006*

xii. *http://en.wikipedia.org/wiki/Sensitivity_and_specificity*